Text and references to accompany Nevada Bureau of Mines and Geology Map 174

Geologic Map of the Caetano Caldera, Lander and Eureka Counties, Nevada

by

Joseph P. Colgan[1], Christopher D. Henry[2], and David A. John[1]

[1]U.S. Geological Survey, Menlo Park, CA 94025
[2]Nevada Bureau of Mines and Geology, University of Nevada, Reno, NV 89557

2011

INTRODUCTION

The Eocene (34 Ma) Caetano caldera in north-central Nevada offers an exceptional opportunity to study the physical and petrogenetic evolution of a large (20 km by 10–18 km pre-extensional dimensions) silicic magma chamber, from precursor magmatism to caldera collapse and intrusion of resurgent plutons. Caldera-related rocks shown on this map include two units of crystal-rich intracaldera tuff totaling over 4 km thickness, caldera collapse breccias, tuff dikes that fed the eruption, hydrothermally altered post-eruption rocks, and two generations of resurgent granitic intrusions (John et al., 2008). The map also depicts middle Miocene (about 16–12 Ma) normal faults and synextensional basins that accommodated >100 percent extension and tilted the caldera into a series of ~40° east-dipping blocks, producing exceptional 3-D exposures of the caldera interior (Colgan et al., 2008).

This 1:75,000-scale map is a compilation of published maps and extensive new mapping by the authors (fig. 1), and supersedes a preliminary 1:100,000-scale map published by Colgan et al. (2008) and John et al. (2008). New mapping focused on the margins of the Caetano caldera, the distribution and lithology of rocks within the caldera, and on the Miocene normal faults and sedimentary basins that record Neogene extensional faulting. The definition of geologic units and their distribution within the caldera is based entirely on new mapping, except in the northern Toiyabe Range, where mapping by Gilluly and Gates (1965) was modified with new field observations. The distribution of pre-Cenozoic rocks outside the caldera was largely compiled from existing sources with minor modifications, with the exception of the northeastern caldera margin (west of the Cortez Hills Mine), which was remapped in the course of this work and published as a stand-alone 1:6000-scale map (Moore and Henry, 2010).

New field mapping was recorded on color 1:24,000-scale aerial photographs and 1:24,000-scale topographic maps; associated data locations were established by handheld GPS units. Field mapping was digitally compiled in ArcGIS using 1:24,000-scale topographic maps, color satellite imagery, and ASTER (Advanced Spaceborne Thermal Emission and Reflection Radiometer) data processed to highlight distinctions between hydrothermally altered versus unaltered volcanic rocks (John et al., 2011). Geologic contacts are shown as solid lines where directly observed in the field and dashed lines where interpreted from aerial photographs or satellite images.

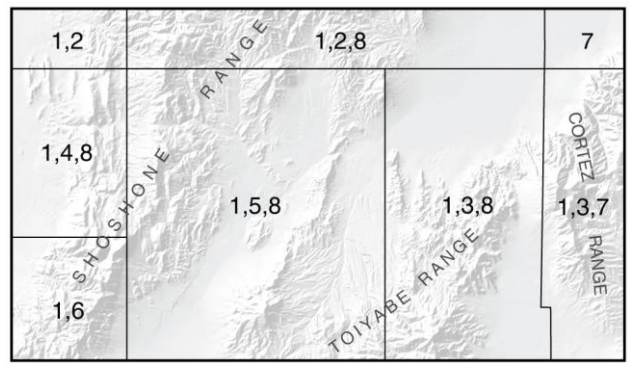

Figure 1. Index map showing sources of geologic map data: (1) This study; (2) Shoshone Range (Gilluly and Gates, 1965); (3) Cortez 15′ quadrangle (Gilluly and Masursky, 1965); (4) The Cedars 15′ quadrangle (McKee and Stewart, 1969); (5) Carico Lake 15′ quadrangle; (6) The Cedars 7.5′ quadrangle (Moore et al., 2005); (7) Roberts et al., 1967 (Eureka County); (8) Stewart and McKee, 1977 (Lander County).

The geologic map is registered to a custom 1:75,000-scale base map with a contour interval of 25 meters. Contours were generated in ArcGIS from 30 m National Elevation Dataset (*ned.usgs.gov*) DEM data using the Spatial Analyst module, and edited by hand to remove artifacts. Cultural features are from the USGS Crescent Valley and Fish Creek Mountains 1:100,000-scale topographic maps, with the exception of new roads and open-pit boundaries in the vicinity of the Pipeline and

Cortez Hills mines, which were delineated by the authors during fieldwork. Mine boundaries are approximately accurate as of September 2010, but continue to evolve.

The margin of the Caetano caldera is shown on the map with a single line symbol, but the nature of this contact differs from place to place. In most places on the map, the caldera margin is a high-angle buttress unconformity—the "topographic" margin of the caldera—formed during caldera collapse as tuff and blocks of wall rock banked against the bedrock scarp that formed the caldera margin. In other places, the caldera margin is a high-angle fault—the "structural" margin of the caldera—formed during caldera collapse as the caldera floor and overlying, earlier-erupted tuff were downfaulted against Paleozoic wall rocks. The northeastern caldera margin west of Cortez Hills consists of two faults. The inner fault (the Copper fault) separates upper-plate Paleozoic rocks from 4-km-thick intracaldera tuff and accommodated most caldera subsidence. The transition up-section from sharp, well-exposed structural margin on the west to buttress unconformity with abundant meso- and megabreccia on the east is well preserved along the Copper fault. Along the outer ring-fracture fault (the Fortress fault), upper-plate Paleozoic rocks subsided against lower-plate rocks while the fault zone served as a conduit for erupting tuff. This complex segment of the caldera margin is shown on a 1:6000 scale geologic map published by Moore and Henry (2010).

Cross section A–A' illustrates the structural style of Miocene normal faulting that broke apart the Caetano caldera. Based on a more detailed study of extensional faulting in the area of this map, Colgan et al. (2008) concluded that the caldera had been extended 22 ± 3 km (110 percent strain). The major source of uncertainty in this estimate is the general lack of dip data for normal faults; based on a compilation of the limited outcrop and map data, Colgan et al. (2008) concluded that middle Miocene normal faults in the area of this map initiated at 60–70º angles. Normal faults on section A–A' were drawn with initial dips in this range, leading to ~105 percent strain when restored. The restored section reveals the post-collapse, early Oligocene geometry of the caldera and demonstrates that caldera subsidence was initially greater in the east, where lower intracaldera tuff is thicker, but subsequently greater in the west, where upper intracaldera tuff is thicker.

DESCRIPTION OF MAP UNITS

Surficial Deposits

m Mine dumps, ponds, and leach pads.

Qp Playa deposits (Quaternary)—Clay, silt, and sand forming surface deposits in ephemeral lake basins in modern valleys.

Qal Alluvium (Quaternary)—Unconsolidated alluvial sand and gravel, and lacustrine deposits in modern stream beds and valleys.

Qaf Alluvial-fan deposits (Quaternary)—Unconsolidated to poorly consolidated deposits of boulders, gravel and sand that form the modern alluvial fans and pediment surfaces mostly developed on Miocene sedimentary rocks.

Miocene Sedimentary and Volcanic Rocks

Ts Sedimentary rocks (Miocene)—Generally poorly exposed sandstone and conglomerate with lesser finer-grained tuffaceous deposits. Mostly light-gray or brown to white, fine- to medium-grained sandstone in beds 10–20 cm thick, containing variable amounts of tuffaceous material including glass shards and crystal and lithic fragments. Sandstones locally interbedded with thin (~10 cm) lenticular beds of conglomerate with 1- to 5-cm clasts of quartzite, chert, and/or volcanic rocks. Thicker conglomerate beds consist of poorly consolidated, light-brown, massively bedded, medium- to fine-grained sandstone containing matrix-supported (locally channelized), angular to subrounded cobbles as much as 50 cm across (generally 1–5 cm). Clasts most commonly consist of white Paleozoic quartzite and black chert and locally of Caetano Tuff. Sandstone and conglomerate interbedded with thinly laminated (<1 cm), white tuffaceous shale and 2- to 5-m thick beds of light-gray to white volcanic ash. Age approximately 16–12 Ma, based on sanidine $^{40}Ar/^{39}Ar$ dates and tephra correlations (Colgan et al., 2008).

Tmr Rhyolite dome (Miocene)—White, gray, and red flow-banded rhyolite with ~2 percent total phenocrysts of sanidine, plagioclase, quartz, and biotite; intrudes Paleozoic rocks and Tertiary gravel (Tg) along crest of Cortez Mountains. Sanidine K-Ar age of 15.6 ± 0.4 Ma (Wells et al., 1969).

Tb Basaltic andesite lava flows (Miocene)—Dark-gray to black lava flows up to 100 m thick on the southeastern crest of the Cortez Mountains. Contain <2 percent fine-grained plagioclase and less abundant clinopyroxene phenocrysts in a pilotaxitic groundmass. Whole-rock $^{40}Ar/^{39}Ar$ ages of 16.36 ± 0.05 and 16.67 ± 0.14 Ma (Colgan et al., 2008).

Tbi Basaltic andesite dikes (Miocene)—Fine-grained diabase dikes in central Cortez Mountains. Contain 2–3 percent plagioclase and trace clinopyroxene phenocrysts in microcrystalline groundmass. Whole-rock $^{40}Ar/^{39}Ar$ age from one dike is 15.4 Ma (R.J. Fleck, unpub. data).

Eocene to Oligocene Rocks Postdating the Caetano Caldera

Tfm Fish Creek Mountains Tuff (Oligocene)—Single exposure in Reese River Valley near western edge of map. Densely welded, crystal-rich (~30 volume percent) rhyolite ash-flow tuff with phenocrysts of sanidine and smoky quartz, sourced from Fish Creek Mountains caldera 10 km west of map area (McKee, 1970). Sanidine $^{40}Ar/^{39}Ar$ age of 24.88 ± 0.05 Ma (John et al., 2008).

Tbu Bates Mountain Tuff, undivided (Oligocene)—Composite map unit composed of rhyolite ash-flow tuffs and locally interbedded sedimentary rocks. Encompasses three genetically unrelated ash-flow tuffs corresponding to units B, C, and D of the Bates Mountain Tuff as defined for exposures at Bates Mountain ~60 km south of the map area (Stewart and McKee, 1968; McKee, 1968; Sargent and McKee, 1969; Grommé et al., 1972).

Tbd D unit of Bates Mountain Tuff (Oligocene)—Mostly densely welded, gray-weathering, pumiceous, and sparsely porphyritic ash-flow tuff containing ~5 percent phenocrysts of sanidine, anorthoclase, plagioclase, and sparse quartz and biotite. Sanidine $^{40}Ar/^{39}Ar$ age of 25.43 ± 0.07 Ma (John et al., 2008). Equivalent to Nine Hill Tuff (Bingler, 1978; Deino, 1989).

Tbc C unit of Bates Mountain Tuff (Oligocene)—Poorly to densely welded, orange-weathering, pumiceous, sparsely porphyritic ash-flow tuff containing about 10 percent fine- to medium-grained phenocrysts of plagioclase, sanidine, prominent embayed (vermicular) quartz, and biotite. Sanidine $^{40}Ar/^{39}Ar$ age of 28.83 ± 0.06 Ma (John et al., 2008). Equivalent to tuff of Campbell Creek (McKee and Conrad, 1987; Henry et al., 2004; Faulds et al., 2005).

Tbb B unit of Bates Mountain Tuff (Oligocene)—Moderately to densely welded, orange-weathering, sparsely pumiceous, moderately porphyritic ash-flow tuff containing phenocrysts of plagioclase, sanidine, and biotite. Sanidine $^{40}Ar/^{39}Ar$ age of 30.67 ± 0.07 Ma (John et al., 2008). Equivalent to tuff of Sutcliffe (Henry et al., 2004; Faulds et al., 2005).

Ttu Plagioclase-biotite tuff (Oligocene)—Crops out in Wilson Canyon and south of Moss Creek. Densely welded ash-flow tuff zoned upward from sparsely to moderately porphyritic with 5–15 percent phenocrysts of sanidine, plagioclase, and biotite. Dense welding and sparse, small pumice make identification as ash-flow tuff difficult. Sanidine $^{40}Ar/^{39}Ar$ age of 30.42±0.04 Ma (table 1).

Tad Andesite and dacite lava flows (Oligocene)—Black to light-gray, locally glassy, finely to coarsely porphyritic andesite and dacite lava flows with phenocrysts of plagioclase and clinopyroxene ± hornblende. Overlies post-caldera sedimentary rocks (Tcs) in western part of caldera. In the southwestern part of the map area includes the "dacite of Wood Canyon," which overlies Caetano Tuff despite a reported age of 34.77 ± 0.10 Ma (Moore and O'Sullivan, 2005).

Tcs Post-caldera sedimentary rocks (Oligocene)—Platy to poorly bedded, gray-green tuffaceous sandstone, siltstone, white shale, minor limestone, and boulder- to pebble-conglomerate containing clasts (to 60 cm) of porphyritic andesite, Caetano Tuff, Bates Mountain Tuff, and Paleozoic rocks. Present within the Caetano caldera, overlying upper unit (Tcu) of Caetano Tuff. Probably deposited in lacustrine, fluvial and (locally) alluvial fan settings.

Tg Boulder- to pebble-conglomerate and sandstone (Miocene(?) to Eocene)—Poorly sorted and moderately to poorly lithified unit deposited unconformably on Paleozoic basement. More than 400 m thick in the southern Cortez Mountains, where it contains blocks up to 10 m across of Paleozoic rock, granitic rock, porphyritic andesite, flow-banded rhyolite, Caetano Tuff, and Bates Mountain Tuff (units C and D). Sanidine $^{40}Ar/^{39}Ar$ age from a reworked ash layer in this deposit is 34.19 ± 0.20 Ma (John et al., 2008). Elsewhere includes conglomerate that overlies Paleozoic rocks and underlies Bates Mountain Tuff along northern caldera margin; contains moderately well-sorted, locally silicified, subangular clasts of chert and quartzite to 10 cm.

Caetano Caldera

Hydrothermally altered rocks—Hydrothermally altered Caetano Tuff and intrusive rocks in western part of caldera. Plagioclase phenocrysts mostly replaced by kaolinite; sanidine is unaltered, perthitic, or replaced by kaolinite or montmorillonite; biotite replaced by kaolinite, montmorillonite, and/or opaque oxides; groundmass replaced by fine-grained silica and/or kaolinite and fine-grained pyrite. Locally, plagioclase and sanidine are leached, leaving prominent voids in a residual quartz matrix. Most pyrite is oxidized. Narrow (generally ≤1 mm), sheeted and stockwork specular hematite veins with prominent hematite-rich silicified vein envelopes are common throughout most of the alteration zone. Coarse-grained barite filling narrow veins and forming breccia matrix is common in southwestern part of caldera west of Carico Lake. Alteration postdates Redrock Canyon porphyry (Tcr) and upper unit of Caetano Tuff (Tcu) and is cut by unaltered Carico Lake pluton (Tcc) (John et al., 2011).

Large Intrusions

Tcc Carico Lake pluton (Eocene)—Porphyritic granite with 50–60 volume percent, 1–5 mm phenocrysts of smoky quartz, sanidine, plagioclase and 2–3 percent biotite and hornblende and trace allanite in a microcrystalline (aplitic) quartz-feldspar groundmass. Rare large sanidine phenocrysts are as much as 2 cm long and poikilitic with numerous plagioclase inclusions. Small miarolitic cavities are common. Contains locally abundant xenoliths of quartzite and pelitic metasedimentary rocks up to 30 cm across. Sanidine $^{40}Ar/^{39}Ar$ age is 34.00 ± 0.05 Ma (John et al., 2008).

Tcr Redrock Canyon porphyry (Eocene)—Medium- to coarse-grained granite porphyry that is pervasively altered and contains 20–30 percent phenocrysts of rounded smoky quartz, mostly altered sanidine and plagioclase up to 1 cm across, and 1–3 percent pervasively altered biotite and hornblende in a felsite groundmass now altered to kaolinite and quartz. Groundmass texture coarsens downward (westward) and deepest exposures have 0.05–0.1 mm aplitic texture. Small miarolitic cavities are common. Sanidine $^{40}Ar/^{39}Ar$ age is 33.90 ± 0.05 Ma.

Small Intrusions

Tci_1 Porphyritic ring-fracture intrusion (Eocene)—Small intrusion along northern caldera margin in northwestern Carico Lake Valley, consisting of granite porphyry with sparse white alkali-feldspar phenocrysts as much as 1 cm long. Contains about 45 percent medium-grained phenocrysts of plagioclase, sanidine, and smoky quartz and 3–5 percent biotite, sparse hornblende, and local orthopyroxene in a glassy to felsitic groundmass. Locally strongly flow-banded. Sanidine $^{40}Ar/^{39}Ar$ age is 33.96 ± 0.06 Ma.

Tci_2 Fine-grained granite porphyry (Eocene)—Small intrusion 2 km northwest of Carico Lake consisting of fine-grained granite porphyry containing about 25–30 percent fine-grained phenocrysts of rounded smoky quartz, sanidine, and plagioclase, and trace amounts of oxidized hornblende in an aphanitic groundmass containing abundant miarolitic cavities.

Tci_3 Flow-banded rhyolite ring-fracture intrusion (Eocene)—Small intrusion on southern caldera margin ~1.5 km north of Red Mountain. Commonly spherulitic, with prominent clay-altered spherulites as much as 4 cm in diameter. Contains 5–10 percent of 1- to 5-mm phenocrysts of clear quartz, and sanidine and plagioclase altered to kaolinite in an aphyric, devitrified, locally flow-banded groundmass pervasively altered to kaolinite and quartz.

Extrusive Rocks

Tct Caetano Tuff, outflow sheet (Eocene)—Densely welded, crystal-rich rhyolite ash-flow tuff identical in composition and age to intracaldera Caetano Tuff (Tcl and Tcu). Up to 250 m thick. Crops out as conspicuous ledges of densely welded, reddish-weathering tuff. Black vitrophyric zones locally present. Sanidine $^{40}Ar/^{39}Ar$ ages are 34.04 ± 0.05 and 33.97 ± 0.06 Ma (John et al., 2008).

Tcb Caetano Tuff, meso- and megabreccia (Eocene)—Mesobreccia is massive to thick-bedded breccia containing clasts up to 2 m in diameter, typically supported by locally tuffaceous matrix of finely comminuted rock fragments. Clasts are predominantly quartzite, chert, and argillite—typical of the lower Paleozoic Roberts Mountains allochthon. Subordinate clasts include rhyolite porphyry, granite, Eocene and Paleozoic limestone, and minor jasperoid in the eastern part of the caldera. Mesobreccia along the southwestern caldera margin (from Red Mountain west to The Cedars) also contains blocks of densely welded Caetano Tuff. Both the upper and lower intracaldera tuff units contain numerous small mesobreccia lenses too small to show at map scale, mostly consisting of pebble-size fragments of chert, quartzite, and argillite. In the northern Toiyabe Range, Gilluly and Gates (1965) mapped these mesobreccia layers as sedimentary rocks (conglomerate) interbedded with Caetano Tuff. Megabreccia occurs along northeastern caldera margin west of the Cortez Hills Mine, and consists of individual blocks or clusters of blocks up to 100 m minimum diameter, mostly of lower Paleozoic chert and argillite, typical of the Roberts Mountains allochthon, with lesser porphyritic rhyolite (Tpr), and sparse clasts of Wenban Limestone. Meso- and megabreccia are inferred to have been deposited by small and large rock falls and massive rock avalanches during and immediately after caldera subsidence (John et al., 2008).

Tcu Caetano Tuff, upper intracaldera unit (Eocene)—Multiple thin cooling units of poorly to densely welded rhyolite ash-flow tuff, locally interbedded with conglomerate, sandstone, and fine-grained platy tuffaceous siltstone. Thin, densely welded vitrophyres are present locally. Crops out as pale-gray to orange, banded slopes punctuated by thin ledges of more resistant welded tuff. Tuffs commonly contain angular fragments of densely welded lower intracaldera Caetano Tuff up to 1.4 m across, and locally contain hornblende-pyroxene andesite and Paleozoic fragments up to 15 cm across. Poorly to moderately welded tuffs are characterized by distinctive orange pumice fragments. About 400 m thick on east side of caldera and up to 1200 m thick in western part of caldera between Carico Lake Valley and Redrock Canyon. Base of unit defined as a prominent topographic break between densely welded, ledge-forming lower intracaldera tuff (Tcl) and poorly welded, slope-forming tuffaceous sandstone and conglomerate at base of upper intracaldera

unit. Tuffs contain about 25–40 volume percent of 1- to 5-mm phenocrysts consisting of smoky quartz, sanidine, and plagioclase with 3–5 percent biotite, hornblende, and local orthopyroxene. Accessory minerals include allanite, zircon, and apatite. Sanidine $^{40}Ar/^{39}Ar$ age is 33.91 ± 0.04 Ma. Mostly hydrothermally altered to quartz-kaolinite-pyrite in the western part of the caldera (John et al., 2011). Even where strongly altered and poorly exposed, this unit can be reliably distinguished from the lower intracaldera cooling unit by the ubiquitous interbedded fine-grained sedimentary rocks.

Tcl Caetano Tuff, lower intracaldera unit (Eocene)—Compound cooling unit of densely welded, crystal-rich rhyolite ash-flow tuff, containing about 35–50 volume percent phenocrysts as much as 5 mm in maximum dimension. Quartz, sanidine, and plagioclase form >90 percent total phenocrysts. Distinctive quartz phenocrysts are dark-gray to black (smoky) and partly resorbed. Total mafic mineral suite, generally <4 volume percent, consists principally of biotite and scarce opaque minerals, but includes minor hornblende and trace orthopyroxene in some places. Accessory minerals include euhedral allanite crystals up to 1 mm long, apatite, and zircon. Strongly flattened pumice blocks are crystal-rich, but less commonly only sparsely porphyritic, and contain phenocryst assemblages similar to the matrix. Exposed thickness as great as 3400 m in the Toiyabe Range. Weighted mean of nine sanidine $^{40}Ar/^{39}Ar$ ages is 34.02 ±0.05 Ma (John et al., 2008). Hydrothermally altered in the western part of the caldera. Mostly hydrothermally altered to quartz-kaolinite-pyrite in the western part of the caldera (John et al., 2011). A 10- to 20-m-thick basal vitrophyre is preserved along the caldera floor in the northern Toiyabe Range, and numerous thin vitrophyric zones envelop beds of mesobreccia or zones of tuff rich in lithic clasts.

Feeder Dike

Tcf Caetano Tuff, composite feeder dike (Eocene)—Composite dike of sparsely porphyritic rhyolite cut by abundantly porphyritic rhyolite tuff, both emplaced along the outer ring fracture of the northeastern caldera margin. Both phases contain same phenocryst assemblage as—and are compositionally indistinguishable from—the lower intracaldera Caetano Tuff (Tcl). Tuff phase of dike is abundantly porphyritic and contains abundant to sparse fragments of lower Paleozoic rocks typical of the Roberts Mountains allochthon, and of porphyritic rhyolite (Tpr) up to ~25 cm in diameter, both in a variably disaggregated (tuffaceous) matrix. Tuff phase strongly flow-banded near margins, but flow bands disaggregate into individual flattened pumice blocks inward. Rhyolite phase is massive to locally flow-banded. Interpreted as feeder dikes for erupted Caetano Tuff based on phenocrysts, composition, and age. Ages, sparsely porphyritic rhyolite: 34.01 ± 0.06 Ma (sanidine $^{40}Ar/^{39}Ar$), rhyolite tuff: 34.00 ± 0.05 and 33.98 ± 0.06 Ma (sanidine $^{40}Ar/^{39}Ar$).

Cenozoic Rocks Predating the Caetano Caldera

Tcm Tuff of Cove Mine (Eocene)—Crystal-rich rhyolite ash-flow tuff underlying lower intracaldera Caetano Tuff at one locality ~3 km southwest of Horse Mountain on the northwestern caldera margin. Contains phenocrysts of quartz, sanidine, plagioclase, biotite, and hornblende. Distinguished from the petrographically similar Caetano Tuff by greater total mafic mineral (6–10 volume percent) and plagioclase contents. Typically contains 5–8 volume percent biotite and 1–2 percent hornblende. Weighted mean of four sanidine $^{40}Ar/^{39}Ar$ ages is 34.44 ± 0.01 Ma (John et al., 2008).

Tpr Porphyritic rhyolite dikes, sills, breccia dikes, domes, and minor tuff (Eocene)—Includes both high- and low-silica rhyolite. High-silica rhyolite contains 10–20 percent phenocrysts of quartz, sanidine, plagioclase, and biotite, up to about 2 mm in diameter. Low-silica rhyolite contains ~30 percent phenocrysts of plagioclase, biotite, and quartz up to about 5 mm long. Forms massive to flow-banded, devitrified to vitrophyric intrusions near the Cortez Hills gold deposit and the rhyolite dome to the southeast in the Cortez Mountains. Breccia dikes contain abundant, rounded to angular clasts of rhyolite up to ~1 m in diameter and sparse to abundant Paleozoic rock fragments in a dark matrix composed mostly of finely ground Paleozoic rock with common small rhyolite clasts and phenocryst fragments. Drill core and exposures in the Cortez Hills pit indicate breccia dikes are the upper, explosively brecciated parts of porphyritic rhyolite dikes. Variably pumiceous and lithic tuff with similar phenocryst assemblage as—and containing sparse to abundant clasts of—the porphyritic rhyolite. This tuff forms an irregular, 300- to 400-m-wide megabreccia block just south of the northeastern caldera margin west of Cortez Hills. Rhyolite is one of the dominant clasts in intracaldera megabreccia, suggesting that numerous rhyolite dikes had intruded Paleozoic rocks near the caldera margin prior to caldera collapse. Age: 35.69 ± 0.06 Ma, mean of 13 sanidine $^{40}Ar/^{39}Ar$ analyses.

Toa Andesite lava (Eocene)—Porphyritic andesite lava flows and block and ash flows exposed on caldera floor between Caetano Ranch and Wenban Spring in the Toiyabe Range. Phenocrysts mostly 0.25–2 mm plagioclase and clinopyroxene, with local hornblende. Mostly devitrified and weakly propylitized. Plagioclase $^{40}Ar/^{39}Ar$ age is 35.21 ± 0.18 Ma.

Tfv Volcanics rocks of Fye Canyon (Eocene)—Andesitic and dacitic lava flows, block and ash flows, and intrusions and rhyolite lava flows and domes exposed in southeasternmost corner of map area. Rhyolite plagioclase $^{40}Ar/^{39}Ar$ ages are 35.73 ± 0.06 Ma and 35.82 ± 0.12 Ma,

and andesite plagioclase age is $^{40}Ar/^{39}Ar$ age 34.92 ± 0.37 Ma.

Tob Basaltic lava flows (Eocene)—Dark-gray, weakly propylitized, fine-grained, sparsely porphyritic plagioclase-pyroxene basalt lava flows on the floor of the Caetano caldera ~3 km southwest of Horse Mountain near the northwestern caldera margin. Undated but stratigraphically below the tuff of Cove Mine.

Td Porphyritic dacite (Eocene)—A single dike of porphyritic dacite crops out just east of the Crescent Valley fault ~3 km southwest of the Cortez mines. Contains 1- to 5-mm phenocrysts of plagioclase, biotite, quartz, and hornblende. Biotite $^{40}Ar/^{39}Ar$ age is 38.90 ± 0.11 Ma, and U-Pb zircon age is 38.93 ± 0.32 Ma. The dike, truncated at the caldera margin, is about 60 m long and as much as 10 m wide. Plagioclase and hornblende phenocrysts are altered to calcite and chalcedony.

Tl Limestone (Eocene)—Fine-grained, white, beige, and locally iron-stained orange to reddish-brown, fetid limestone underlying gravel deposits (unit Tg) and outflow sheet of Caetano Tuff near Horse Canyon in the Cortez Mountains. Locally contains small chert nodules. Locally coarsely recrystallized with dark reddish-brown hematitic gossan layers.

Tog Conglomerate and sandstone (Eocene)—Exposed on the caldera floor near Wenban Spring, along the southeastern caldera margin in the Toiyabe Range, where it is massive to well-bedded and calcite-cemented with angular to subrounded clasts of Paleozoic limestone, chert, and minor quartzite to 90 cm. Conodonts from a limestone clast in this section span the Silurian to the Mississippian (A.G. Harris, written communication reported in John et al., 2008), consistent with lower Paleozoic limestone derived from the lower plate of the Roberts Mountains allochthon. Also forms part of caldera floor on northwest edge of Toiyabe Range, where lithified conglomerate contains subrounded clasts of quartzite, chert, argillite, granite, diorite, and flow-banded rhyolite as much as 1.5 m in diameter in a sandy noncalcareous matrix.

Mesozoic Intrusive Rocks

Jgr Mill Canyon stock and dikes (Jurassic)—Probable composite intrusion and nearby dikes. Consists of biotite quartz monzonite (locally with plagioclase phenocrysts), granodiorite, porphyritic rhyolite, and lamprophyre. Age is 158.4±0.6 Ma (zircon U-Pb; TIMS; Mortensen et al., 2000).

Paleozoic Rocks

Pzh Havallah sequence (Golconda allochthon) (Permian to Devonian)—Argillite, chert, sandstone, and siltstone in the southwestern part of the map area (Moore et al., 2005).

Pzo Antler overlap assemblage (Permian to Pennsylvanian)—Rocks deposited in angular unconformity on the Roberts Mountains allochthon. Includes predominantly clastic rocks of the Permian Horseshoe Basin sequence (Racheboeuf et al., 2004) and the Pennsylvanian and Permian Cedars sequence (Moore et al., 2000). Includes dark-red chert-pebble conglomerate forming floor of Caetano caldera near Caetano Ranch in the Toiyabe Range (John et al., 2008).

Pzrm Roberts Mountains allochthon (Devonian to Ordovician)—Argillite, chert, quartzite, sandstone, greenstone, and minor limestone. Includes rocks assigned to the Valmy Formation, Vinini Formation, Elder Sandstone, and Slaven Chert (Gilluly and Gates, 1965; Gilluly and Masursky, 1965).

Pzlc Lower plate of Roberts Mountains allochthon (Devonian to Cambrian)—Limestone, dolomite, quartzite, and shale in the plate of the Roberts Mountains thrust. Includes rocks assigned to the Wenban Limestone, Roberts Mountains Formation, Hanson Creek Formation, Eureka Quartzite, and Hamburg Dolomite (Gilluly and Gates, 1965; Gilluly and Masursky, 1965).

ACKNOWLEDGMENTS

We thank Bob Leonardson of Barrick Gold Corp. for access to the Cortez and Pipeline mine areas, and for drill-core samples from the Cortez Hills area. $^{40}Ar/^{39}Ar$ ages were determined at the New Mexico Geochronology Research Laboratory (New Mexico Institute of Mining and Technology) under the patient guidance of Bill McIntosh, Matt Heizler, Lisa Peters, and Rich Esser. The first draft of this map was significantly improved following reviews by Ed du Bray, Keith Howard, John Muntean, and Kathryn Watts.

REFERENCES

Bingler, E.C., 1978, Abandonment of the name Hartford Hill Rhyolite Tuff and adoption of new formation names for middle Tertiary ash-flow tuffs in the Carson City–Silver City area, Nevada: U.S. Geological Survey Bulletin, 1457-D, 19 p.

Colgan, J.P., John, D.A., Henry, C.D., and Fleck, R.J., 2008, Large-magnitude Miocene extension of the Eocene Caetano caldera, Shoshone and Toiyabe Ranges, Nevada: Geosphere, v. 4, no. 1, p. 107–130, doi:10.1130/GES00115.1.

Deino, A.L., 1989, Single crystal $^{40}Ar/^{39}Ar$ dating as an aid in correlation of ash flows—examples from the Chimney Springs/New Pass Tuffs and the Nine Hill/Bates Mountain Tuffs of California and Nevada: New Mexico Bureau of Mines and Mineral Resources Continental Magmatism Abstracts Bulletin, v. 131, p. 70.

Faulds, J.E., Henry, C.D., and Hinz, N.H., 2005, Kinematics of the northern Walker Lane—an incipient transform fault along the Pacific–North American plate boundary: Geology, v. 33, no. 6, p. 505–508, doi: 10.1130/G21274.1.

Gilluly, J., and Gates, O., 1965, Tectonic and igneous geology of the northern Shoshone Range, Nevada, *with sections on* Gravity survey of part of Crescent Valley, by D. Plouff, *and* Economic geology, by K.B. Ketner: U.S. Geological Survey Professional Paper 465, 153 p.

Gilluly, J., and Masursky, H., 1965, Geology of the Cortez quadrangle, Nevada: U.S. Geological Survey Bulletin 1175, 117 p., 3 plates.

Gonsior, Z.J., 2006, The timing and evolution of Cenozoic extensional normal faulting in the southern Tobin Range, Pershing County, Nevada: Nevada Bureau of Mines and Geology Open-File Report 06-4, 64 p.

Gonsior, Z.J., and Dilles, J.H., 2008, Timing and evolution of Cenozoic extensional normal faulting and magmatism in the southern Tobin Range, Nevada: Geosphere, v. 4, no. 4, p. 687–712.

Grommé, C.S., McKee, E.H., and Blake, M.C., Jr., 1972, Paleomagnetic correlations and potassium-argon dating of middle Tertiary ash-flow sheets in the eastern Great Basin, Nevada and Utah: Geological Society of America Bulletin, v. 83, no. 6, p. 1619–1638, doi: 10.1130/0016-7606(1972)83[1619:PCAPDO]2.0.CO;2.

Henry, C.D., Faulds, J.E., dePolo, C.M., and Davis, D.A., 2004, Geology of the Dogskin Mountain quadrangle, Washoe County, Nevada: Nevada Bureau of Mines and Geology Map 148, scale 1:24,000, 20 p.

John, D.A., Henry, C.D., and Colgan, J.P., 2008, Magmatic and tectonic evolution of the Caetano caldera, north-central Nevada—a tilted mid-Tertiary eruptive center and source of the Caetano Tuff: Geosphere, v. 4, no. 1, p.75–106, doi: 10.1130/GES00116.1.

John, D.A., Rockwell, B.W., Henry, C.D., and Colgan, J.P., 2011, Hydrothermal alteration of the late Eocene Caetano ash-flow caldera, north-central Nevada—a field and ASTER remote sensing study, *in* Steininger, R., and Pennell, B., editors, Great Basin evolution and metallogeny: Geological Society of Nevada 2010 Symposium Proceedings, Reno, Nevada, May 14–22, 2010, v. 2, p. 1055-1083.

Kuiper, K.F., Deino, A., Hilgen, F.J., Krijgsman, W., Renne, P.R., and Wijbrans, J.R., 2008, Synchronizing rock clocks of Earth history: Science, v. 320, no. 5875, p. 500–504.

McIntosh, W.C., Heizler, M., Peters, L., and Esser, R., 2003, $^{40}Ar/^{39}Ar$ geochronology at the New Mexico Bureau of Geology and Mineral Resources: New Mexico Bureau of Geology and Mineral Resources Open File Report OF-AR-1, 10 p.

McKee, E.H., 1968, Geologic map of the Spencer Hot Springs quadrangle, Lander County, Nevada: U.S. Geological Survey Geologic Quadrangle Map GQ-770, scale 1:62,500.

McKee, E.H., 1970, Fish Creek Mountains Tuff and volcanic center, Lander County, Nevada: U.S. Geological Survey Professional Paper 681, 17 p.

McKee, E.H., and Conrad, J.E., 1987, Geologic map of the Desatoya Mountains Wilderness Study Area, Churchill and Lander counties, Nevada: U. S. Geological Survey Miscellaneous Field Studies Map MF-1944, scale 1:62,500.

McKee, E.H., and Stewart, J.H., 1969, Geologic map of The Cedars quadrangle, Lander County, Nevada: U.S. Geological Survey Open-File Report 69-158, scale 1:62,500.

Moore, S.C., and Henry, C.D., 2010, Preliminary geologic map of the northeastern margin of the Caetano caldera, Lander County, Nevada: Nevada Bureau of Mines and Geology Open-File Report 10-10, scale 1:6000.

Moore, T.E., and O'Sullivan, P.B., 2005, Miocene gold mineralization and exhumation in the southern Shoshone Range, north-central Nevada, *in* Rhoden, N.H., Steininger, R.C., and Vikre, P.G., editors, Symposium 2005—window to the world: Geological Society of Nevada Symposium Proceedings, Reno/Sparks, Nevada, May 14-18, 2005, v. 1, p. 103–123.

Moore, T.E., Murchey, B.L., and Harris, A.G., 2000, Significance of geologic and biostratigraphic relations between the overlap assemblage and Havallah sequence, southern Shoshone Range, Nevada, *in* Cluer, J.K., Price, J.G., Struhsacker, E.M., Hardyman, R.F., and Morris, C.L., editors, Geology and ore deposits 2000—the Great Basin and beyond: Geological Society of Nevada Symposium Proceedings, Reno/Sparks, Nevada, May 15–18, 2000, v. 1, p. 397–418.

Mortensen, J.K., Thompson, J.F.H., and Tosdal, R.M., 2000, U-Pb age constraints on magmatism and mineralization in the northern Great Basin, Nevada, *in* Cluer, J.K., Price, J.G., Struhsacker, E.M., Hardyman, R.F., and Morris, C.L., editors, Geology and ore deposits 2000—the Great Basin and beyond: Geological Society of Nevada Symposium Proceedings, Reno/Sparks, Nevada, May 15–18, 2000, v. 1, p. 419–438.

Racheboeuf, P.R., Moore, T.E., and Blodgett, R.B., 2004, A new species of *Dyoros* (Brachiopoda, Chonetoidea) from Nevada (United States) and stratigraphic implications for the Pennsylvanian and Permian Antler overlap assemblage: Geobios, v. 37, no. 3, p. 382–394.

Renne, P.R., Swisher, C.C., Deino, A.L., Karner, D.B., Owens, T.L., and DePaolo, D.J., 1998, Intercalibration of standards, absolute ages and uncertainties in $^{40}Ar/^{39}Ar$ dating: Chemical Geology, v. 145, p. 117–152, doi: 10.1016/S0009-2541(97)00159-9.

Roberts, R.J., Montgomery, K.M., and Lehner, R.E., 1967, Geology and mineral resources of Eureka County, Nevada: Nevada Bureau of Mines and Geology Bulletin 64, 164 p., scale 1:250,000.

Sargent, K.A., and McKee, E.H., 1969, The Bates Mountain Tuff in northern Nye County, Nevada: U.S. Geological Survey Bulletin 1294-E, 12 p.

Steiger, R.H., and Jäger, E., 1977, Subcommission on geochronology—convention on the use of decay constants in geo- and cosmochronology: Earth and Planetary Science Letters, v. 36, no. 3, p. 359–362.

Stewart, J.H., and McKee, E.H., 1968, Geologic map of the Mount Callaghan quadrangle, Lander County, Nevada: U.S.

Geological Survey Geologic Quadrangle Map GQ-730, scale 1:62,500.
Stewart, J.H., and McKee, E.H., 1969, Geology of the Carico Lake quadrangle, Lander County, Nevada: U.S. Geological Survey Open-File Report 69-268, scale 1:62,500.
Stewart, J.H., McKee, E.H., and Stager, H.K., 1977, Geology and mineral deposits of Lander County, Nevada: Nevada Bureau of Mines and Geology Bulletin 88, 114 p., scale 1:250,000.
Wells, J.D., Stoiser, L.R., and Elliot, J.E., 1969, Geology and geochemistry of the Cortez gold deposit: Economic Geology, v. 64, no. 5, p. 526–537.

Suggested citation:

Colgan, J.P., Henry, C.D., and John, D.A., 2011, Geologic map of the Caetano caldera, Lander and Eureka counties, Nevada: Nevada Bureau of Mines and Geology Map 174, scale 1:75,000, 10 p.

Table 1. $^{40}Ar/^{39}Ar$ ages of igneous rocks in the Caetano caldera area.

Laser-Fusion Analyses	Sample #	Min[1]	**Age (28.02)**	±2σ	**Age (28.201)**	K/Ca	±2σ	n[2]	Latitude	Longitude	Reference
Miocene Tephra											
Reworked tephra; 5920 bench, Cortez Hills pit	H09-139	an	**10.8**	0.2	**10.9**	11	4	3	40.16958	-116.60219	New
Tephra, Wilson Canyon section	JC06-CT121	san	**15.03**	0.10	**15.13**	8.5	3.5	6	40.21278	-116.92194	Colgan et al., 2008
Tephra, NW Carico Lake Valley	H05-62	san	**15.21**	0.07	**15.31**	7.2	4.2	6	40.17583	-116.81667	Colgan et al., 2008
Tephra; 1094 ft depth, DC99-15 drill hole	DC99-15 1094	an	**15.24**	0.17	**15.34**	9	2	2	40.15778	-116.61000	John et al., 2008
Tephra, base of Wilson Canyon section	JC06-CT116	an	**15.38**	0.30	**15.48**	9.6	15.5	5	40.21305	-116.92194	Colgan et al., 2008
Tephra, base of Moss Creek section	JC06-CT120	an	**15.68**	0.14	**15.78**	1.7	0.4	6	40.21972	-117.00638	Colgan et al., 2008
Tephra along "tuff fault," South Gap pit	JC09-CT322	an	**15.7**	0.2	**15.8**	3	5	3	40.24828	-116.72423	New
Tephra, base of Moss Creek section	JC06-CT107	an	**15.84**	0.15	**15.94**	1.7	0.5	4	40.21778	-117.00722	Colgan et al., 2008
Pyroclastic-fall tuff, Pipeline pit	CJV2	an	**15.88**	0.10	**15.98**	1.6	1	8	40.24977	-116.72157	John et al., 2008
Tephra, NE of Red Mountain	JC08-CT203	san	**16.4**	0.3	**16.5**	64	174	3	40.10222	-116.82525	New
Post-Caetano Ash-Flow Tuffs											
Fish Creek Mountains Tuff	H03-73	san	**24.72**	0.05	**24.88**	21.0	6.8	15	40.18627	-117.24263	John et al., 2008
"Plagioclase-biotite tuff"	H06-39	san	**30.23**	0.04	**30.42**	31.1	3.6	8	40.22645	-116.92929	New
Bates Mountain Tuffs, Reese River Narrows & New Pass											
D Nine Hill Tuff, New Pass	H00-78	san	**25.27**	0.07	**25.43**	9.4	2.5	15	39.57637	-117.52721	John et al., 2008
C tuff of Campbell Creek	H01-139	san	**28.64**	0.07	**28.83**	55.7	13.4	10	39.94438	-117.14159	John et al., 2008
B tuff of Sutcliffe	H01-138	san	**30.48**	0.06	**30.67**	31.7	4.3	15	39.94491	-117.14183	John et al., 2008
A tuff of Rattlesnake Canyon	H01-137	san	**31.03**	0.07	**31.23**	38.3	4.2	12	39.94438	-117.14296	John et al., 2008
Caetano Caldera											
Post-collapse intrusions											
Carico Lake intrusion	H03-96	san	**33.78**	0.05	**34.00**	55.7	16.2	15	40.16722	-116.84862	John et al., 2008
Red Rock Canyon intrusion	07-DJ-12	san	**33.68**	0.05	**33.90**	58	15.0	19	40.14125	-116.90211	New
Ring-fracture intrusion	06-DJ-82	san	**33.74**	0.06	**33.96**	14	63.0	22	40.21358	-116.85914	New
Intracaldera tuff											
Tilted section, Cortez 15' quadrangle, Toiyabe Range											
Highest exposed	00-DJ-34	san	**33.79**	0.08	**34.01**	78.7	35.2	12	40.15633	-116.62136	John et al., 2008
Highest exposed	00-DJ-34	san	**33.81**	0.05	**34.03**	61.1	35.5	14	40.15633	-116.62136	John et al., 2008
Middle exposed	H03-82	san	**33.82**	0.05	**34.04**	69.4	24.5	13	40.15868	-116.66343	John et al., 2008
Lowest exposed	H03-84	san	**33.71**	0.07	**33.92**	82.9	32.6	10	40.16440	-116.67692	John et al., 2008
Other intracaldera											
Upper unit, Tub Spring section	08-DJ-88B	san	**33.69**	0.04	**33.91**	62	23.0	15	40.11828	-116.82280	New
Moss Creek Canyon, uppermost	H03-94	san	**33.74**	0.05	**33.96**	69.5	21.1	14	40.20753	-117.02875	John et al., 2008
Moss Creek Canyon, lowermost	05-DJ-14	san	**33.84**	0.08	**34.06**	58.9	27.1	10	40.20856	-117.03818	John et al., 2008
South of Rocky Pass, lowermost	05-DJ-27	san	**33.85**	0.09	**34.07**	63.4	33.4	10	40.17145	-116.81544	John et al., 2008
The Cedars quadrangle	H03-88B	san	**33.81**	0.08	**34.03**	82.5	29.9	9	40.11700	-117.03700	John et al., 2008
Caetano Tuff dike, Fortress fault											
Sparsely porphyritic rhyolite dike	H07-52	san	**33.79**	0.06	**34.01**	92	24.0	15	40.17456	-116.64711	New
Abundantly porphyritic rhyolite tuff dike	CH05-102 2150	san	**33.76**	0.06	**33.98**	57	20.0	7	40.16670	-116.63079	New
Abundantly porphyritic rhyolite tuff dike	H07-55B	san	**33.78**	0.05	**34.00**	84	30.0	14	40.17627	-116.65528	New
Outflow tuff related to intracaldera tuff											
The Cedars quadrangle, Shoshone Range	H03-89	san	**33.83**	0.05	**34.04**	58.7	25.8	21	40.09663	-117.05763	John et al., 2008
Golconda Canyon, Tobin Range	Tru5-4	san	**33.75**	0.06	**33.97**	--	--	10	40.32450	-117.59367	Gonsior, 2006; John et al., 2008
Reworked pyroclastic-fall tuff											
Horse Canyon, Cortez Mountains	99-DJ-80	san	**33.97**	0.20	**34.19**	--	--	--	40.13181	-116.52264	John et al., 2008
Tuff of Cove Mine											
Base of section, Wilson Pass	06-DJ-13	san	**34.21**	0.10	**34.43**	63.8	16.6	7	40.25761	-116.97843	John et al., 2008
Elephant Head, south of Battle Mountain	H03-87	san	**34.21**	0.07	**34.43**	--	--	9	40.60825	-116.98945	John et al., 2008
Northern Fish Creek Mountains	05-DJ-8	san	**34.22**	0.06	**34.45**	81.2	14.0	9	40.41410	-117.21910	John et al., 2008
Mule Canyon quadrangle	H00-53	san	**34.23**	0.09	**34.45**	62.0	12.4	13	40.56940	-116.70849	John et al., 2008
Mule Canyon quadrangle	98-DJ-52	san	**34.45**	0.08	**34.67**	--	--	--	40.52222	-116.71694	John et al., 2000
Fye Canyon Volcanics											
Rhyolite lava	09-DJ-84	plag	**35.50**	0.06	**35.73**	2.5	5.1	5	40.02626	-116.48719	New
Rhyolite lava	09-DJ-90	plag	**35.59**	0.12	**35.82**	0.6	0.7	7	40.02096	-116.53115	New

(continued on next page)

Table 1. $^{40}Ar/^{39}Ar$ ages of igneous rocks in the Caetano caldera area—*Continued.*

Step-Heating Analyses	Sample #	Min[1]	**Age (28.02)**	±2σ	**Age (28.201)**	K/Ca	±2σ	%^{39}Ar	Latitude	Longitude	Reference
Pre-caldera andesite lava, Caetano Ranch area	H05-52	plag	**34.98**	0.18	**35.21**	0.14	0.1	78	40.12672	-116.68442	New
Andesite plug, Fye Canyon volcanics	09-DJ-87	plag	**34.70**	0.37	**34.92**	0.24	0.3	72	40.02374	-116.53732	New
Porphyritic dacite dike, north margin of caldera	H08-17	bio	**38.65**	0.11	**38.90**	12.9	15	88	40.16687	-116.67303	New
Jurassic lamprophyre dike, Cortez Mountains	H09-145	hbl	**159.44**	0.44	**160.5**	0.13	0	92.4	40.20045	-116.55392	New

[1]Min = Mineral analyzed: an = anorthoclase, san = sanidine, plag = plagioclase, bio = biotite, hbl = hornblende

[2] *n* = Number of individual grains used to define weighted mean age. %^{39}Ar = percentage of ^{39}Ar used to define plateau age

Decay constants and isotopic abundances after Steiger and Jäger (1977); $\lambda_\beta = 4.963 \times 10^{-10}$ yr^{-1}; $\lambda_{\varepsilon+\varepsilon'} = 0.581 \times 10^{-10}$ yr^{-1}; $^{40}K/K = 1.167 \times 10^{-4}$

Minerals were separated from crushed, sieved samples by standard magnetic and density methods; sanidine was leached with 5% HF to remove matrix and handpicked. Most analyses at the New Mexico Geochronological Research Laboratory (methods in McIntosh et al., 2003). Samples were irradiated in Al discs for 7 hours in D-3 position, Nuclear Science Center, College Station, TX. Single sanidine grains were fused with a CO_2 laser operating at 10 W. Extracted gases were purified with SAES GP-50 getters. Argon was analyzed with a Mass Analyzer Products (MAP) model 215-50 mass spectrometer operated in static mode. Neutron flux monitor Fish Canyon Tuff sanidine (FC-1) with assigned ages of 28.02 Ma (Renne et al., 1998) and 28.201 Ma (Kuiper et al., 2008).

Leader (--) indicates no data.